Simultaneous use of PIV and UVP to measure velocity profiles and turbulence in jet flow.

A. H. Rabenjafimanantsoa[a], Rune W. Time[a] and Arild Saasen[b]

[a]University of Stavanger, NO-4036 Stavanger, Norway
[b]Statoil ASA, NO-4035 Stavanger Norway

ABSTRACT

The development of self-organized coherent structures formed by liquid particle jet flow has been studied experimentally. Liquid particle flow issued from a round turbulent jet was studied by application of simultaneous PIV and UVP recordings. Both Newtonian and non-Newtonian fluids have been used as flowing medium. The non-Newtonian fluids consisted of blends of polyanionic cellulose (PAC) and fresh water. Their viscosity profiles are presented to discuss effects of viscosity on the jet-flow pattern. The jet-flow configuration field is well suited to compare the instruments performance, and contains complex structures encountered in practical hydraulic applications.

There was reasonable agreement between quantitative measurements of the velocity profiles and turbulence intensities measured by UVP and PIV techniques.

INTRODUCTION

A simple experimental flow facility was constructed to study the dynamics of a liquid jet entering a liquid filled transparent cell. Small glass spheres suspended in the liquid in the cell serve both to interact with the turbulent flow and as seeding particles for UVP and PIV.

Ultrasound velocity profile (UVP) monitoring can be used to measure flow velocity and turbulence intensity via suspended seed particles. The velocities measured by UVP and PIV are not the fluid velocities directly but the velocities of the particles suspended in the fluid. UVP has the advantage of being applicable where a requirement for measurement of opaque flows and non intrusive systems is to be considered.

PIV is now widely used for flows where there is an optical access. It gives the instantaneous two-dimensional, two- or three-component velocity vector field with high accuracy and high spatial and temporal resolution[1]. PIV techniques require transparent flow conditions to capture particle images.

Turbulent liquid pipe flows laden with particles (or solids) occurs in a wide range of engineering applications ranging from particle transport in the petroleum industry to radioactive waste transport. It has therefore been a goal for researchers to develop models for particle dispersion by turbulence and turbulence attenuation by particles. A priori the path of the particles is not known, thus it is difficult to estimate the fluid velocity of the surrounding fluid.

Jet flow has been widely studied through theory, experiment and numerical simulation. It occurs in numerous applications and the geometry is also simple to set up in experiments. The flow is separated by three regions with their respective character[2]. Dispersion of particles in a jet flow will help to characterize the flow and identify the induced self organized coherent motions.

The structure of a particle-laden round jets has been studied experimentally by Longmire and Eaton[3]. They found that the near field of the particle-laden jet was dominated by axisymmetric vortex ring structures which were rolling up in the shear layer. In addition, their flow visualization studies showed that the particle dispersion was dominated by the coherent structures.

Solid-liquid transport in pipes occurs in a wide range of engineering applications. In this respect, it is important to understand the mixing process where the flow is dominated by turbulent transport.

Particles form beds at sufficiently low flow velocities, typically in the range of 0.2 - 0.5 m/s. The current work is expanding on the works of Rabenjafimanantsoa et al.[4,5] involving dunes and ripples formations in hydraulic transport of particles. In this work only UVP technique was used to study the turbulent flow and pressure variations above mobile particles bed.

As mentioned dispersions of solid liquid are common in drilling and production in the oil industry. In perspective of the complex mixture behavior, the modelling of the specific properties is not easy.

In this study we focus on simultaneous measurements of particle velocity measurements on dispersions using combined PIV and UVP techniques. Data and images were processed using a modified version of a Matlab-based software (The MathWorks, Inc), MatPIV[6].

EXPERIMENTAL

The experimental configuration in the study of jet flow is presented in Fig. 1.

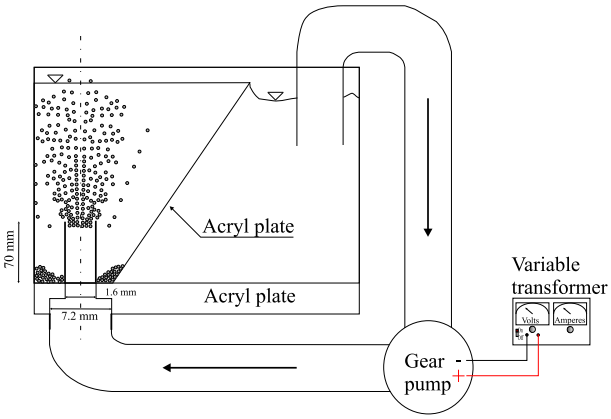

Figure 1: Schematic of the jet flow configuration

Four glass plates were assembled to form the rectangular glass cell used for the experiments. The cell was mounted on an acrylic ground plate which was placed on two tables that could be lifted manually. The jet flow was formed by the nozzle through the acrylic plate. The nozzle diameter was 1.6 mm and is situated 25 mm from the left side of the glass wall. The water jet dragged the particles through a short circular flow straightener pipe of D = 10 mm in diameter. The flow straightener was set to decrease the Coanda effect, i.e. flow being attracted to the wall. The main flow was driven by a gear pump which was controlled using a variable transformer. An acrylic plate was placed as seen from Fig. 1 to prevent particles from being sucked in into the pump. We used flexible tubing both upstream and downstream of the pump to avoid pump vibrations which could disturb the flow.

The instrumental set up is presented in Fig. 2. The UVP instrument from Met-Flow[7] is described by Rabenjafimanantsoa et al.[5]. The starting channel was set to 5 mm and the distance between channels 0.74 mm. The instrument measures velocity profiles from channel 0 to channel 127 in 1000 profiles. The measurement window length is then the sum of the starting channel and the product of window end-channel with the channel distance. The beam angle was set to 78^o from horizontal. However, the PIV instrument has been successfully tested with different systems before implemented in this study. The primary components are a double-pulsed laser sheet and a HiSense PIV/PLIF camera, from Dantec Dynamics with spatial resolution of 1024x1280 pixels, which are synchronized by a PC. The camera objective was a Nikon Micro-Nikkor 60/2.8. For the camera to work with the

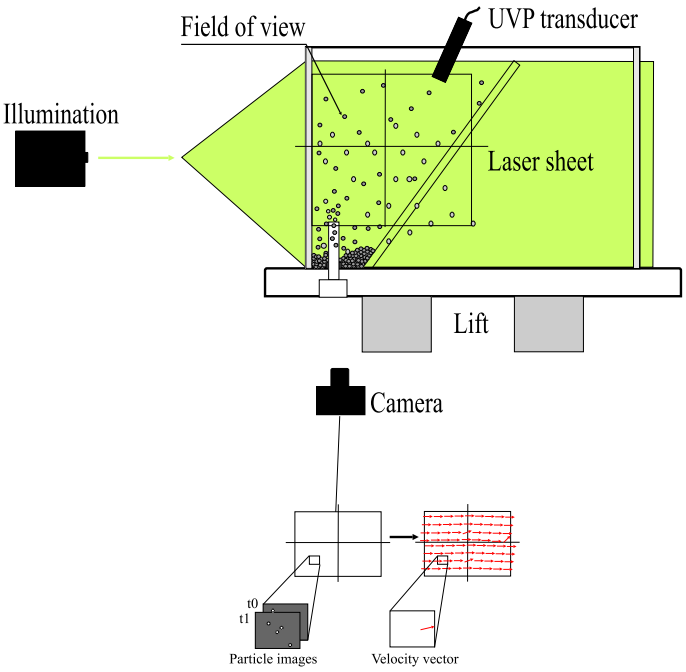

Figure 2: Schematic arrangement of the instruments

FlowMap©PIV 1500 processor system, the FlowManager version 4.1 software was used to allow postprocessing of the images. The illumination source was a pair of Solo Nd:YAG laser (from New Wave Research, Inc.). The laser delivered 106 mJ energy at 532 nm wavelength. The laser sheet with a sufficient thickness illuminated the flow. The camera position shown in Fig. 2 is situated 70 cm perpendicular to the glass cell. The laser sheets are formed by sending the laser beams through cylindrical lenses, and then into the measured region. The field of view is selected by the camera position and lens parameters. One experimental take-up with the PIV consists of 10 "recordings". Each recording consists of a two exposures (frames). The time interval between the double frames is 1 ms, and the time interval between the recordings is 500 ms.

The synchronization of the UVP and PIV was needed for correct comparison of data from the instruments. This was accomplished by simultaneous triggering of the UVP and PIV. The UVP was triggered externally with the BNC line from the camera which sent TTL signals. The UVP recording was longer than the PIV sequence in order to obtain improved statistics for velocity profile and turbulence.

As seeding particles for both PIV and UVP glass beads with a density of 2.52 g/cc and ranging between 250 and 300 μm were used. They were added initially from the top of the rectangular glass cell and remained recirculating in the fluid chamber.

As expected polyanionic cellulose (PAC) seems to have a weak effect as drag reducing agent. Two different concentrations were used: 200 and 400 ppm dissolved in water. These were chosen because we got nearly constant viscosities with only small drag reducing effect. A mixer (Silverson L4RT-A at 5000 rpm) was used to prepare the solution before pouring into the glass cell. A filter was set to avoid particles from being circulated through the pump. A satisfactory polymer distribution was achieved after 30 minute's recirculation time. The rheological measurements were taken using a Physica UDS 200 rheometer with cone plate configuration MK 24 (75 mm, 1^o) . The two samples were measured at 20^oC with increasing shear rates. The viscosities were measured at three seconds intervals. The following plot (Fig. 3) shows the results from the two different PAC solutions. It can be seen that the solutions are showing shear thinning behavior.

JET DYNAMICS

A jet flow is characterized by three regions[2]. These regions are illustrated in Fig. 4. The first region is called the potential core region or the near field region which is a cone-shaped region. This region starts at the nozzle exit and has a length of 4 to 5 nozzle diameters. The flow then changes to free jet flow characterized by the absences of a potential core and uniform velocity distribution. The last region is characterized by the flow stagnation or the far field region. In this region the velocity decreases.

Between the jet and the surrounding particle laden liquid turbulence oc-

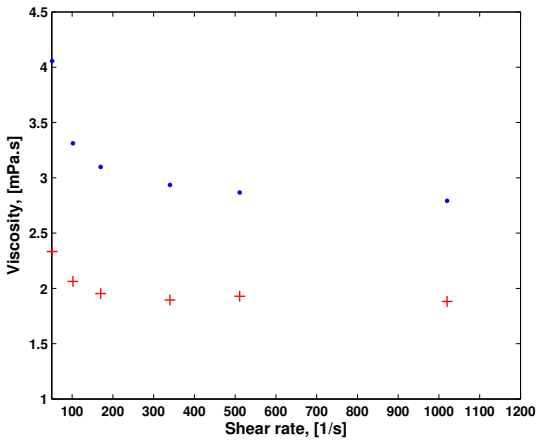

Figure 3: Viscosity versus shear rate at 20^o: the blue · is for 400 ppm PAC while the red + is for 200 ppm PAC

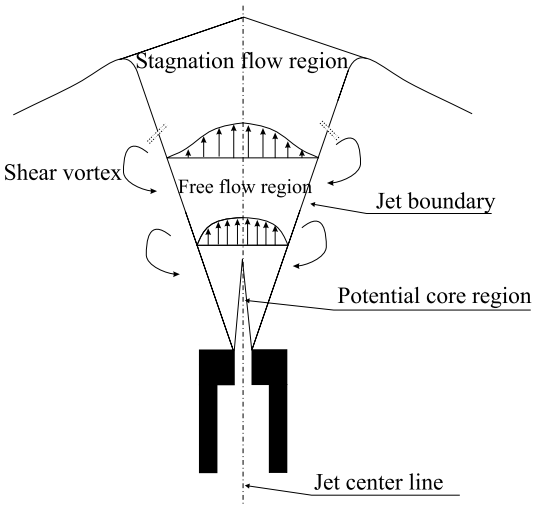

Figure 4: Jet illustration

cur. This is the result of Kelvin-Helmholtz instability due to the velocity differences between the fluid and the surrounding stream. The neighboring fluid layers are drawn by the particles into the motion. Large scale structures influence the mixing and entrainment process[3]. The jet impingement is on a free surface which is an air liquid interface. As a consequence unstable phenomena like oscillation on the free surface can be expected.

RESULTS AND DISCUSSIONS

PIV vs. UVP

We use a Cartesian coordinate system (X,Y) as seen in Fig. 5. The positive X-axis points from left to right and Y-axis points to the streamwise direction (from bottom to top). The origin (0,0) is at the left bottom corner of the image. This corresponds to the bottom left-hand pixel in the camera image. The image coordinate is measured in pixels.

Simultaneous applications PIV and UVP to study jet flow for both Newtonian and non-Newtonian flowing medium has been carried out.

Newtonian flow

We will first present the results obtained from water (i.e. Newtonian flow) to serve as a basis and reference for the non-Newtonian fluid.

Fig. 5 shows a snapshot of the jet image. From this figure the UVP transducer is immersed in the glass cell and transmits the ultrasonic beam from a distance X from the Y-axis. From Fig. 6, at first glance,

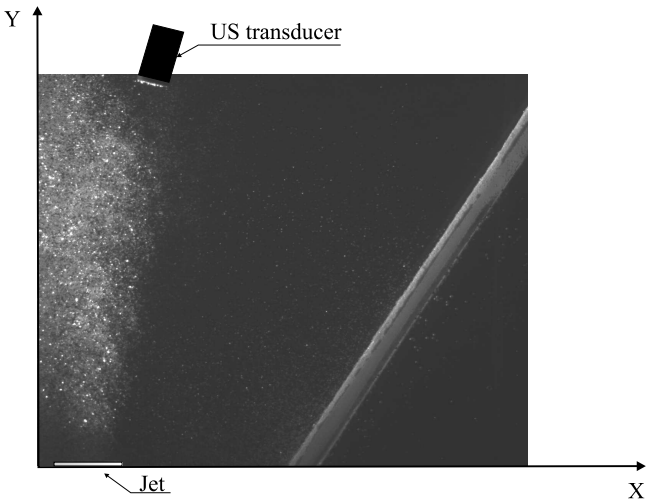

Figure 5: Typical raw PIV image showing the jet behavior and ultrasound transducer placement.

the liquid particles jet flow is diverging. The velocity magnitude together with the

velocity vectors are plotted in the same Fig. 6. The colorbar is in mm/s. Both

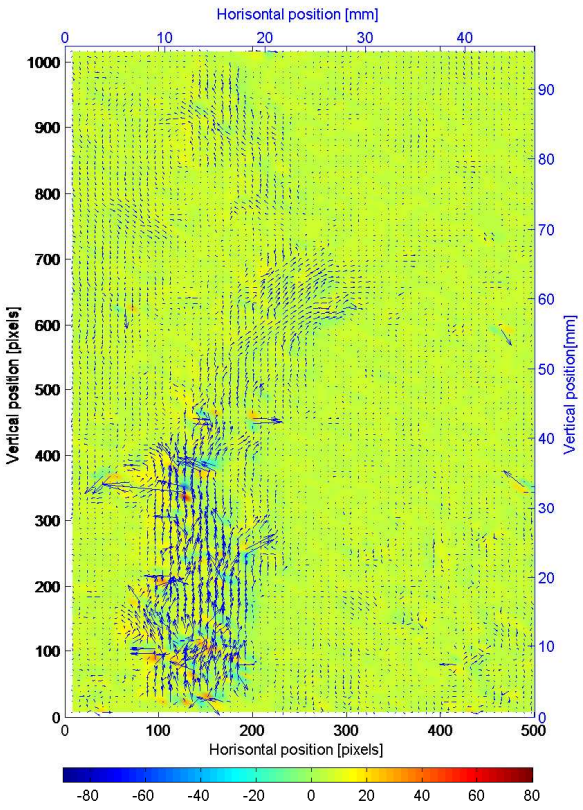

Figure 6: Velocity vector and velocity magnitude results in Newtonian flow from Fig. 5. The colorbar is in mm/s.

values in pixel and real world coordinates are presented. The vectors represent particles directions and velocities which were averaged from their 8 neighboring velocities. The velocity magnitude is color coded where dark blue represents low velocity magnitude while red represents high velocity magnitude. We will focus solely on the main flow.

Although the flow rate totally was insufficient to disperse the particles, the three distinct regions can still be observed. The fluid layer where the velocity changes significantly is referred to as the mixing layer, as reported in many literature. The jet inlet is situated between pixel interval 100 and 200 in the horizontal position axis. From vertical position:

1. between 0 and 200 pixels: the potential core of the jet with uniform velocities. Just downstream of the nozzle exit most of the particles are concentrated here. The jet flow is interacting with the surrounding fluid and exhibit vortical structures at the jet edges.

2. from 200 to 450 pixels: the free flow region. The particles stream break up and their paths are diverted.

3. from 450 to 1000 pixels: the far field or the stagnant flow region. Particles are drawn away from the jet center line.

The distribution or entrainment of particles is also shown in Fig. 6 starting from a very high concentration of particles (in region 1) to a low particle concentration (in region 3). This is the near-field area with respect to the jet flow. The liquid particle flow field is constant except at the position (120,100) pixel where an undulated flow starts growing. Vortex formations are already formed in this initial part of the jet. The high shear rate around the jet occurs in a thin shear layer as revealed by the high and low velocity magnitude, blue color beside red or yellow colors in Fig. 6. This leads to strong turbulent fluctuations. From the same figure the shear layer thickness continues to grow upward as the jet velocity decreases. It is obvious that the mixing process is enhanced in this region.

In region 2 the interaction between liquid and the particles is appearing. Due to vortex break-up the liquid particles flow become complex and unstable but large structures can be observed. From the figure the velocity vectors show undulating patterns that give rise to rotating large scale vortices. These vortex structures have established to start in this region and the jet is widening upwards. As these vortices roll around there are fluid trapped in and incorporate with the surrounding flow.

In the far field or stagnation flow region (region 3) the particles are spread by turbulent diffusion. The jet strength decays and widens due to the deceleration of the liquid particle. The velocity vectors show shorter length. It can be seen that the vor-

tex size is much smaller that in the other regions. Particle entrainment is reduced. They are more dispersed in the fluid and spread horizontally.

Velocity measurements in both X and Y-directions along the ultrasonic measuring line were computed and compared to the velocity profiles results from both instruments. We compute the streamwise velocity profile components of PIV and UVP. Fig. 7 shows the variations of the liquid particle jet flow along the beam in Y-direction. The streamwise velocity profiles

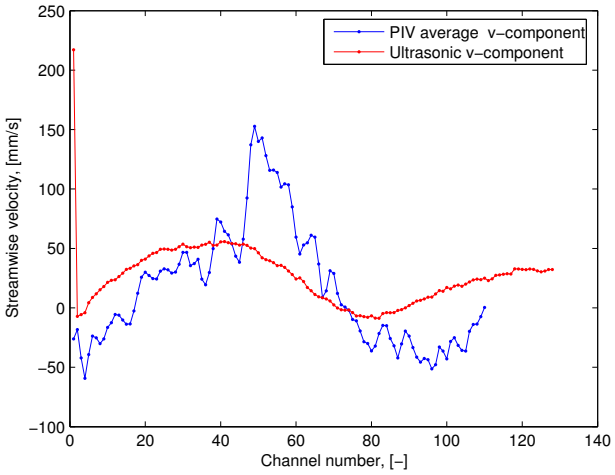

Figure 7: Comparison of time averaged streamwise velocity for PIV and UVP along the beam line. The blue line is the PIV velocity while the red line is the UVP velocity computed from Fig. 6.

of both PIV and UVP is increasing monotonically and reach their respective local maximum. Then, both profiles decrease monotonically with the beam line length. The large difference is that PIV shows higher maximum value probably showing the jet centerline.

Since both instruments were synchronized and measure the same velocity, we obtained comparable instantaneous PIV and UVP velocity profiles. The time needed for the UVP to record one profile was 101 ms. The recorded UVP velocity profiles was analyzed individually and compared with one PIV image pairs.

Fig. 8 shows the comparison between the instantaneous PIV and UVP velocity profiles along the UVP measuring lines. This plot was taken from the same PIV

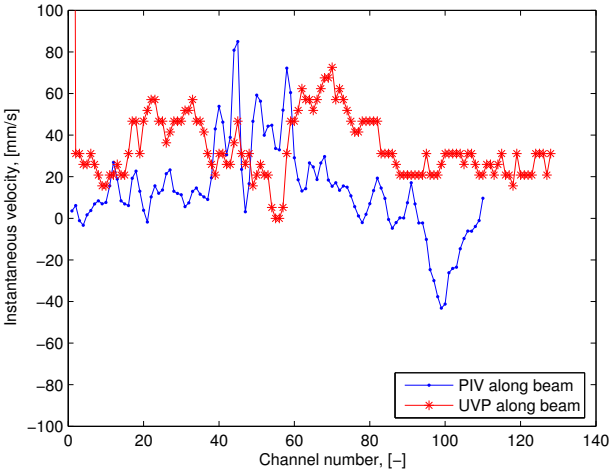

Figure 8: Comparison of instantaneous velocity profiles for PIV and UVP. The blue line is the PIV velocity profile while the red line is the UVP velocity profile computed from Fig. 6.

image pair as in the foregoing figures. The UVP velocity profile is from profile number 4. The two velocity profiles show similar trends except from at the jet centerline. This plot suggests also the position of the jet flow boundaries which could be at channels approximately 40 and 80. A higher UVP velocity profile is observed from the US beam near field area up to approximately channel 40 followed by a decrease in the free flow region of the jet flow. Outside of the jet boundary the UVP velocity profile is increasing to a local maximum before flattening out.

From the near field area of the UVP (i.e. channel 0 to approximately channel 40) the PIV velocity profiles are slightly positive. In this region the concentration of particles were probably not sufficient to give representative velocities. The PIV velocity profile is increasing to a local maximum. Then, from approximately channel 40 to 60, PIV velocity is decreasing while UVP velocity profile is increasing. In this region a high particle flux is occurring and give good representation of PIV velocity

profile.

From channel number 70 on, the PIV velocity profile is negative and a local minimum is observed.

Non-Newtonian flow with PAC 200

However, by adding 200 ppm of PAC to the flowing medium a more pronounced undulation jet flow structure is observed. The vortex structures were dampened as seen in Fig. 9. In turn, the particles were more dispersed outside the jet main flow. This suggests that the surrounding medium keeps the particles in suspension in a more effective way, probably because of increased viscosity. We can see that the jet spreading width is significantly reduced compared to the case of pure water. It could indicate a decrease in turbulent diffusion. From

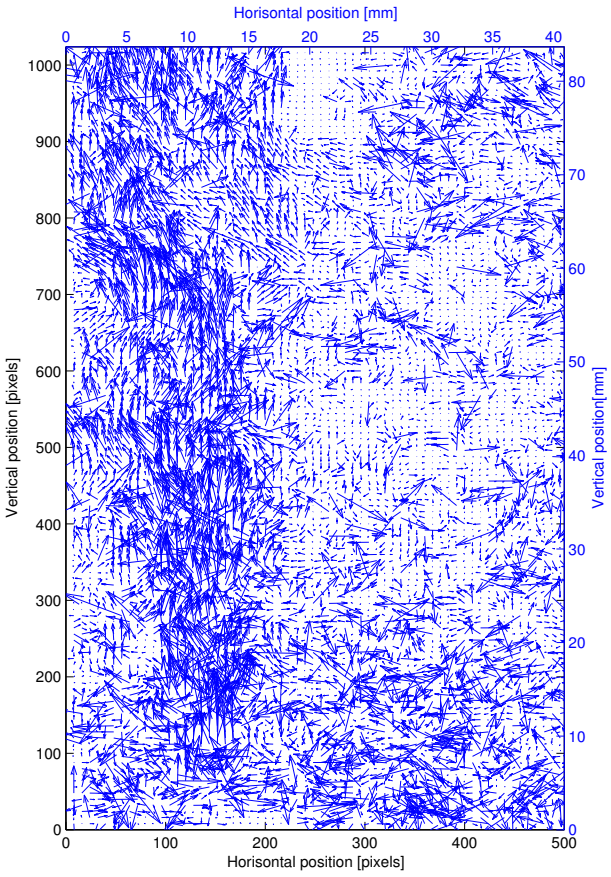

Figure 9: Velocity vector in non-Newtonian flow using 200 ppm PAC.

Fig. 9 the jet is situated between pixel interval 100 and 200 in the horizontal position axis.

An effective way to characterize the different layers is to plot the velocity contour. Fig. 10 shows that there is a large velocity difference over the shear layer. Further away the velocity gradient is lower. As the solution is forced out of the jet nozzle the effect of the polymer is likely to occur giving the stretched pattern of the jet.

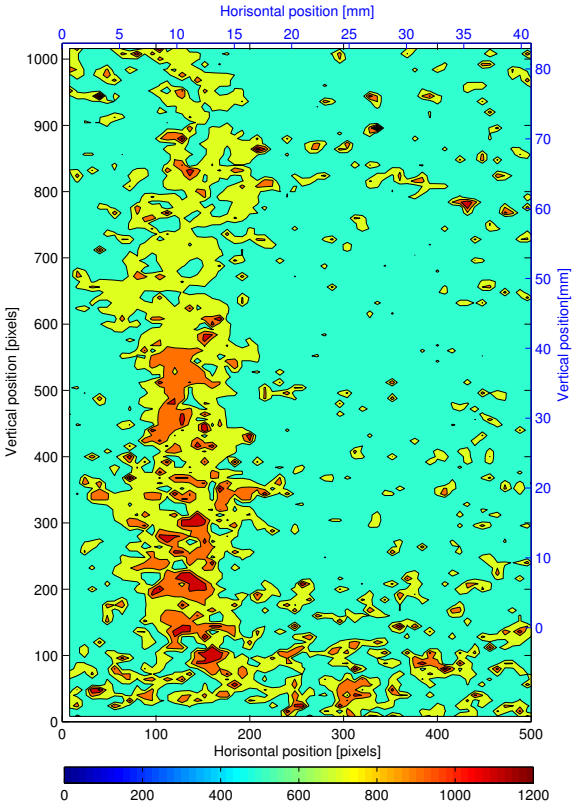

Figure 10: Velocity contours for non-Newtonian flow using 200 ppm PAC. Color scale: 0 represents -140 mm/s and 1200 represents 220 mm/s.

Fig. 11 shows a comparison of the streamwise velocity profiles along the beam line. The plot exhibits a similar trend with increasing velocities starting from the beam's near field area. From approximately channel number 30 the PIV streamwise velocity profile show a fluctuating behavior due to the high concentration of particles. The UVP velocity profile reaches its maximum at channel number 60 and de-

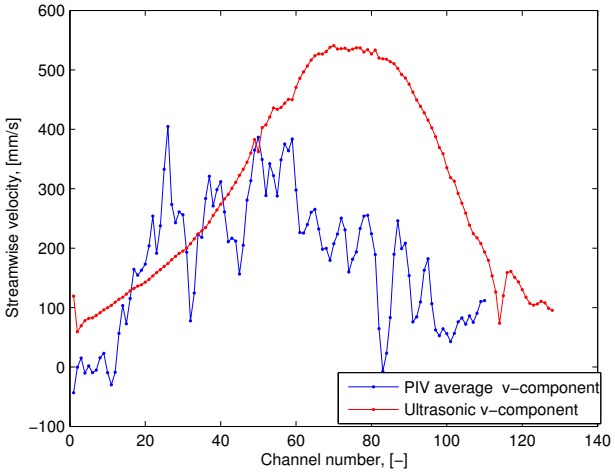

Figure 11: Comparison of the streamwise velocities for PIV and UVP along the beam line for PAC 200. The blue line (·) is the PIV velocity profile while the red line (+) is the UVP velocity profile.

creases outwards.

As mentioned ten image pairs of PIV were acquired ending at UVP profile number 24. The following plot (Fig. 12) shows the same PIV's second image pair as for the foregoing figures, compared to the UVP profile 6. From Fig. 12 the

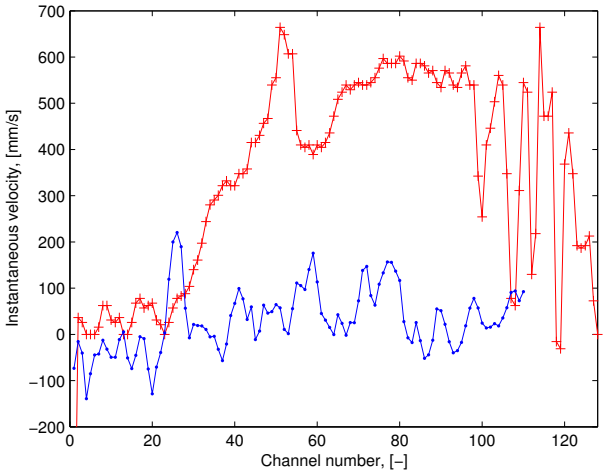

Figure 12: Comparison of instantaneous velocity profiles for PIV and UVP for PAC 200 solution. The blue line is the PIV velocity profile while the red lines are the UVP velocity profile.

UVP velocity profiles start increasing to a sudden peak value at channel number approximately 50. This could be the intersection of the ultrasonic beam with the undulated jet flow. The profiles are distorted with a high velocity zone occurring at the undulated jet. Clouds of particles were flowing upwards causing substantial acoustic attenuation. Under such conditions the UVP has problem to establish representative velocity profiles.

Non-Newtonian flow with PAC 400

Similar performance as for PAC 200 was experienced with PAC 400. Both PIV and UVP velocity profiles were plotted together for comparison. It was observed that the averaged UVP profiles were higher than the averaged PIV profile. The Y-component of the PIV velocity profiles, however, showed good overlap with the UVP velocity profile before the beam was transversing the jet centerline.

CONCLUSIONS

Self-organized structures formed by liquid particle jet flow have been addressed. We studied the complementary aspects of PIV and UVP and gained more information about the flow structures. The experimental configuration is a liquid particle flow issued from a turbulent jet from beneath. Three types of fluids were used: water as Newtonian fluid and two different weakly non-Newtonian solution consisting of PAC dissolved in water.

The analysis demonstrate that with a small amount of polymer solution the jet dynamics are affected. The fluids viscosity tend to stabilize the flow and the self-organized structures were dampened. When using Newtonian fluid the jet dynamic is diverging upwards while for non-Newtonian fluid a reduced jet spreading width was observed. Agreement of the velocity profiles were observed before the UVP transducer beam crossed the jet flow.

Care should be taken when using UVP with fluid having a high concentration of

particles. The beam can be strongly attenuated so that the instrument may become unable to establish representative velocity profiles.

ACKNOWLEDGEMENTS

The work was carried out at the Two Phase Flow Laboratory at the University of Stavanger, Norway. The authors would like to thank Helge Hodne for his help with the rheological measurements.

REFERENCES

1. R. J. Adrian (2005), "Twenty years of particle image velocimetry", Experiments in fluid, Vol. 39, pp. 159-169.

2. Hughes W. F. and Brighton J. A. (1967), "Fluid Dynamics." Shaum′s outline series. McGraw-Hill Book Company.

3. Longmire, E.K., and Eaton, J.K., (1992), "Structure of a Particle-Laden Round Jet", J. Fluid Mechanics, vol. 236, pp. 217-257.

4. Rabenjafimanantsoa, A. H., Time, R. and Saasen, A. (2005), "Flow regimes over particles beds - Experimental Studies of Particle Transport in Horizontal Pipes", Annual Transactions of the Nordic Rheology Society, vol. 13, pp. 99 - 106.

5. Rabenjafimanantsoa, A. H., Time, R., Hana, M. and Saasen, A. (2005), "Dunes Dynamics and Turbulence structures over particle beds - Experimental Studies and Numerical Simulations". Annual Transactions of the Nordic Rheology Society, vol. 13, pp. 171 - 176.

6. An Introduction to MatPIV, ver. 1.6.1. Eprint no. 2, ISSN 0809-4403, Department of Mathematics, University of Oslo. http://www.math.uio.no/∼jks/matpiv/.

7. Met-Flow (2000), "UVP Monitor Model UVP-XW, 2000. User's guide - Met-Flow SA"